NJC

PAPER

Shear disassembly of hierarchical superparamagnetic Fe_3O_4 hollow nanoparticle necklace chains†

Cite this: *New J. Chem.*, 2014, **38**, 6125

Shouhu Xuan,[ab] Lingyun Hao[c] and Ken Cham-Fai Leung*[ad]

Received (in Montpellier, France) 18th June 2014,
Accepted 29th September 2014

DOI: 10.1039/c4nj01005a

www.rsc.org/njc

Supramolecular amide hydrogen-bond interactions between bundles of necklace-like chains based on superparamagnetic hollow Fe_3O_4 nanoparticle beads could be indirectly quantified by shear stress and magnetorheological analyses. First, a facile magnetic field-induced method was developed for the preparation of the superparamagnetic Fe_3O_4 hierarchical chain structures. Primary Fe_3O_4 hollow nanospheres, hollow nanosphere-assembled chains, and partially hollow nanosphere-assembled chains were successfully prepared. These superparamagnetic nanoparticles and chains could be well dispersed in aqueous solutions. The magnetic hollow nanoparticle chains possess a strong magnetorheological effect in aqueous solutions. Bundle wire-like structures based on chains or nanospheres could be formed with different magnetic field alignments. The hollow nanostructure greatly strengthens the as-formed bundle wire-like structures such that the chains have a larger magnetorheological effect than that of the hollow nanospheres. It is envisaged that a specific cell transfection mechanism of chains and wires could involve a partial disassembly from bundles to individual chains/wires before endocytosis. The force that is exerted on this disassembly from bundles to individual chains/wires in a specific medium, which are quantified by shear stress and magnetorheological analyses, would shed light on cell magnetofection mechanisms.

1. Introduction

Magnetic fluids that were composed of magnetic and porous nano/micro-particles dispersed within various types of biological media would be beneficial for effective drug delivery.[1–4] It is well known that endocytosis takes place for transfecting spherical and rod-like nanostructures to specific cells.[5–8] However, long chains and wire-like structures are far less studied in terms of their cell transfection efficiencies.[9] The cell transfection mechanism of chains and wires should involve a partial disassembly from bundles to individual chains/wires to begin with. The force that is exerted on this disassembly from bundles to individual chains/wires in a specific medium could be quantified by shear stress analysis. Moreover, magnetorheological analysis of superparamagnetic chain/wire structures would shed light on magnetofection mechanisms.[7,8] Magnetorheological fluids,[10–12] which possess structure-dependent mechanical properties, show target-controllable transport behavior.[13,14] The viscosity of the magnetic fluids often exhibited a controllable change with an external magnetic field due to the formation of fibrous particle aggregates over the Brownian motion.[15] Different from individual spherical particles, the anisotropic magnetic dispersing phase reduced the settling of particles and thereby increased the magnetorheological effects of the magnetic fluids.[16,17]

Superparamagnetic magnetite (Fe_3O_4) particles can be a conventional option as a magnetic ferrofluid since zero residue magnetic force could be attained upon removing the external magnetic field.[18–20] The rheological properties of the Fe_3O_4 nano/micro-particle fluids play important roles in mechanical and theranostic research. This is because the stability and viscosity of fluids can be tunable by an externally applied magnetic field, thereby leading to a desired response (drug delivery, hyperthermia, *etc.*) in targeted areas. In consideration of the unique advantages of the anisotropic nanostructures, spherical, rod-like, and sheet-like Fe_3O_4 particles were favorable as magnetic fluids.[21–25] The magnetic field-induced method was found to be the most matured fabrication method for synthesizing anisotropic magnetic particles with rod, wire, micro-fiber, and necklace structures.[26–31] Although many other methods such as post-hydrogen reduction, *in situ* decomposition–oxidation methods, the pulsed laser

[a] *Department of Chemistry and Partner State Key Laboratory of Environment and Biological Analysis, Hong Kong Baptist University, Kowloon, Hong Kong SAR, P. R. China. E-mail: cfleung@hkbu.edu.hk*
[b] *CAS Key Laboratory of Mechanical Behavior and Design of Materials, Department of Modern Mechanics, University of Science and Technology of China, Hefei, 230026, P. R. China*
[c] *School of Materials Science and Engineering, Jinling Institute of Technology, Nanjing, 211169, P. R. China*
[d] *Institute of Molecular Functional Materials, University Grants Committee, Hong Kong SAR, P. R. China*

† Electronic supplementary information (ESI) available. See DOI: 10.1039/c4nj01005a

deposition technique, co-polymerization, and DNA templating were also effective for synthesizing the spindle, peanut-like, tubular micro-particle, necklace-like chain and wire structures,[32–36] one-step fabrication of the superparamagnetic Fe_3O_4 particles with a large aspect ratio is still a challenge.

Recently, the one-dimensional magnetic nanostructures were proven to be useful for enhancing their rheological properties but the detailed mechanism still deserves further investigation. Previous reports indicated that several superparamagnetic Fe_3O_4 particle structures could be used as magnetic fluids and carriers, in magnetic targeting therapy and hyperthermia.[36–39] Recently, hollow structured Fe_3O_4 particles were found to be attractive in various applications due to their specific dispersity, quick response to the external field, and large surface areas.[40,41] Only a few papers reported on the particle assembly to form 1-D hierarchical nanostructures.[42–44] In consideration of the importance of the hollow nature[45] to encapsulate more drug molecules and the specific 1-D structure of the dispersing particles in the ferrofluids, facile and scalable synthesis of the 1-D superparamagnetic Fe_3O_4 chain structures based on hollow nanospheres and their structure-dependent rheological properties in the fluid are reported herein.

Specifically, superparamagnetic Fe_3O_4 chains which were assembled by hollow nanospheres were facilely prepared such that they can be further dispersed into aqueous solution to form a new class of magnetic fluids. In comparison to the Fe_3O_4 hollow nanospheres, the 1-D chains lead to a higher magnetorheological effect in aqueous solution. The formation and magnetorheological effect of these Fe_3O_4 chains were discussed with proposed mechanisms.

2. Experimental

Materials

Ferric chloride hexahydrate ($FeCl_3{\cdot}6H_2O$), sodium citrate, urea, polyacrylamide (PAM), poly(acrylic acid) (PAA), sodium acetate, diethylene glycol (DEG), ethylene glycol (EG), and poly(vinylpyrrolidone) (PVP, 30 kDa) of analytical grade were purchased from Sinopharm Chemical Reagent Co, Ltd. All reagents were used as received without further purification. Deionized water was used for all experiments.

Synthesis of Fe_3O_4 hollow nanospheres

In a typical synthesis, 1 mmol of $FeCl_3{\cdot}6H_2O$, 2 mmol of sodium citrate, 3 mmol of urea, 0.15 g of PAM, and 0.1 g of PVP were dissolved in 20 mL of water. After vigorous stirring, the solution was transferred to a Teflon-lined stainless-steel autoclave (25 mL volume) and then sealed to heat at 200 °C. After the reaction, the autoclave was cooled to room temperature and the residues were washed with water and ethanol, and then dried in a vacuum to form a black powder. In this synthesis, two final products were obtained after reactions for 12 and 24 h, respectively. Finally, the products were dispersed into aqueous solution to form the magnetic fluids at different concentrations.

Synthesis of Fe_3O_4 chains based on hollow nanospheres

In a typical synthesis, 1 mmol of $FeCl_3{\cdot}6H_2O$, 2 mmol of sodium citrate, 3 mmol of urea, 0.15 g of PAM, and 0.1 g of PVP were dissolved in 20 mL of water. After vigorous stirring, the solution was transferred to a Teflon-lined stainless-steel autoclave (25 mL volume), placing a small magnet at the bottom, and then sealed to heat at 200 °C. After reaction, the autoclave was cooled to room temperature and the residues were washed with water and ethanol, and then dried in a vacuum to form a black powder. In this synthesis, two final products were obtained after reactions for 12 and 24 h, respectively. Finally, the products were dispersed into aqueous solution to form the magnetic fluids at different concentrations.

Synthesis of Fe_3O_4 partially hollow nanospheres

In a typical synthesis, 1 mmol of $FeCl_3{\cdot}6H_2O$, 2 mmol of sodium citrate, 3 mmol of urea, 0.15 g of PAM, and 0.1 g of PVP were dissolved in 20 mL of water. After vigorous stirring, the solution was transferred to a Teflon-lined stainless-steel autoclave (25 mL volume) and then sealed to heat at 200 °C. After reaction, the autoclave was cooled to room temperature and the residues were washed with water and ethanol, and then dried in a vacuum to form a black powder. In this synthesis, the final product was obtained after a reaction for 5 h. Finally, the products were dispersed into aqueous solution to form the magnetic fluids at different concentrations.

Synthesis of Fe_3O_4 chains based on partially hollow nanospheres

In a typical synthesis, 1 mmol of $FeCl_3{\cdot}6H_2O$, 2 mmol of sodium citrate, 3 mmol of urea, 0.15 g of PAM, and 0.1 g of PVP were dissolved in 20 mL of water. After vigorous stirring, the solution was transferred to a Teflon-lined stainless-steel autoclave (25 mL volume), placing a small magnet at the bottom, and then sealed to heat at 200 °C. After reaction, the autoclave was cooled to room temperature and the residues were washed with water and ethanol, and then dried in a vacuum to form a black powder. In this synthesis, the final product was obtained after a reaction for 5 h. Finally, the products were dispersed into aqueous solution to form the magnetic fluids at different concentrations.

Synthesis of Fe_3O_4 non-hollow (solid) nanospheres

In a typical synthesis, $FeCl_3{\cdot}6H_2O$ (0.54 g), sodium acetate (1.5 g), and PAA (1.5 g) were dissolved in 20 mL of EG/DEG (4 : 1 v/v). After vigorous stirring, the solution was transferred to a Teflon-lined stainless-steel autoclave (25 mL volume) and then sealed to heat at 200 °C. After reaction, the autoclave was cooled to room temperature and the residues were washed with water and ethanol, and then dried in a vacuum to form a black powder. In this synthesis, the final product was obtained after a reaction for 10 h. Finally, the products were dispersed into aqueous solution to form the magnetic fluids at different concentrations.

Synthesis of Fe_3O_4 chains based on non-hollow (solid) nanospheres

In a typical synthesis, $FeCl_3{\cdot}6H_2O$ (0.54 g), sodium acetate (1.5 g), and PAA (1.5 g) were dissolved in 20 mL of EG/DEG (4 : 1 v/v). After vigorous stirring, the solution was transferred to a Teflon-lined

stainless-steel autoclave (25 mL volume), placing a small magnet at the bottom, and then sealed to heat at 200 °C. After reaction, the autoclave was cooled to room temperature and the residues were washed with water and ethanol, and then dried in a vacuum to form a black powder. In this synthesis, the final product was obtained after a reaction for 10 h. Finally, the products were dispersed into aqueous solution to form the magnetic fluids at different concentrations.

Rheological property measurement

The dynamic properties of the magnetic fluids were characterized using a commercial rheometer (Physica MCR 301, Anton paar Co., Austria). The obtained nanofluids were placed between two parallel plates and a shear loading was applied on the sample through the rotating plate, which was made of non-permeable material with a 20 mm diameter rotating plate. The rotating plate can also transmit other signals (such as stress, displacement, and strain) by the sensors connected to it. Magnetic field was generated by a built-in coil whereas the intensity of the magnetic field is controlled by the current in the coil. Magnetic induction lines pass through a permeable framework and sample to form a closed magnetic circuit.

Characterization

The powder X-ray diffraction (XRD) patterns of the products were recorded by using Cu Kα radiation (λ = 1.5418 Å) on a Bruker D8 Advance diffractometer equipped with a graphite diffracted beam monochromator. Transmission electron microscopy (TEM) photographs were taken using a high-resolution transmission electron microscope (HRTEM, Tecnai Model JEOL-2100 and JEOL-2010) at an accelerating voltage of 200 kV. The field emission scanning electron microscopy (FE-SEM) images were taken using a JEOL JSM-6700F SEM. Their magnetic properties (*M–H* curve, magnetization (emu per gram of the sample) *versus* magnetic field (Oe)) were measured at room temperature using a MPMS XL magnetometer made by Quantum Design Corp.

3. Results and discussion

Typically, the iron precursor ($FeCl_3$), coordinating reagent (sodium citrate), polymer surfactants (PAM and PVP), and the pH-regulating reagent (urea) were first mixed to form a homogeneous aqueous solution. At higher temperature (200 °C), PAM could be self-agglomerated to form spherical polymer particles which could be stabilized by citrate and urea molecules/ions at the periphery. Then Fe^{3+} ions could be assembled onto the polymer particle surface (Fe-complex) followed by reduction in alkali medium to produce the ultrasmall Fe_3O_4 nanoparticles (Fe-complex/Fe_3O_4, Fig. 1). In a continuous reaction at high temperature for over 12 h, eventually the PAM core could be dissolved in the solvent and leaked out from the Fe-complex/Fe_3O_4 to produce the hollow/porous Fe_3O_4 particles. Partially hollow Fe_3O_4 particles could be produced by a 5 h reaction with the above-mentioned synthetic procedures. Non-hollow (solid) Fe_3O_4 particles[18] were synthesized from which poly(acrylic acid) (PAA) was employed to replace the polyacrylamide in the synthetic procedures described in Fig. 1. In the synthesis with magnetic field, as soon as the ultrasmall Fe_3O_4 nanoparticles were formed on the surface of the Fe-complex and then formed the hollow nanospheres, they could be self-adhered to form chains. Longer chains that are based on hollow nanospheres could be acquired by extending the reaction time in the presence of an external magnetic field.

Fig. 2 shows typical SEM and TEM images of the as-prepared chains obtained after a reaction for 12 h, which are indicated as chain bundles. These chains possess a non-uniform length ranging from one to tens of micrometers. The higher magnification TEM image indicates that these chains were assembled by uniform hollow nanospheres, exhibiting a necklace-like morphology. The average diameters of the hollow nanospheres, partially hollow nanospheres, and the non-hollow (solid) nanospheres are determined to be 220 ± 20, 230 ± 30, and 310 ± 30 nm, respectively. The average width of the hollow nanosphere in the necklace chain is approximately 200–220 nm which is almost the same as the average diameter of the Fe_3O_4 hollow nanospheres (220 ± 20 nm). The crystalline size is approximately 12 nm by XRD measurements (Fig. S5, ESI†). The SEM images also show the standard bundle structure of the Fe_3O_4 chains, whereas the chains are presumably held together by supramolecular [N–H···C–O] hydrogen-bond interactions between their polyacrylamide surfaces. It was reported that by directly applying a magnetic field, the synthesized Fe_3O_4 nanospheres could be physically attached to each other to form chain-like morphology.[31] However, visible inter-particle space was found between the peripheries of Fe_3O_4 hollow spheres.

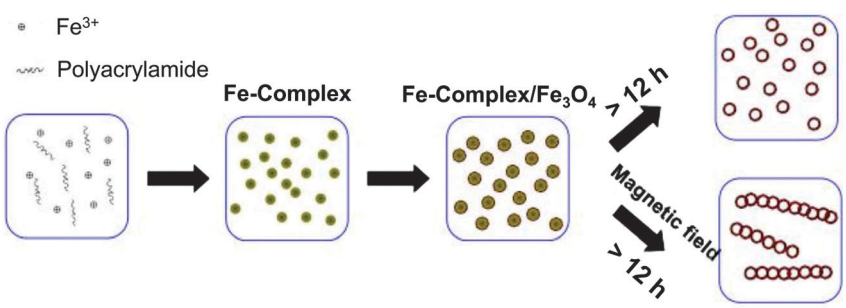

Fig. 1 Scheme showing the synthesis of different products with Fe^{3+} ions and the polyacrylamide surfactant. After reactions for over 12 h, hollow Fe_3O_4 nanospheres and Fe_3O_4 chains based on hollow nanospheres were synthesized without and with magnetic field, respectively.

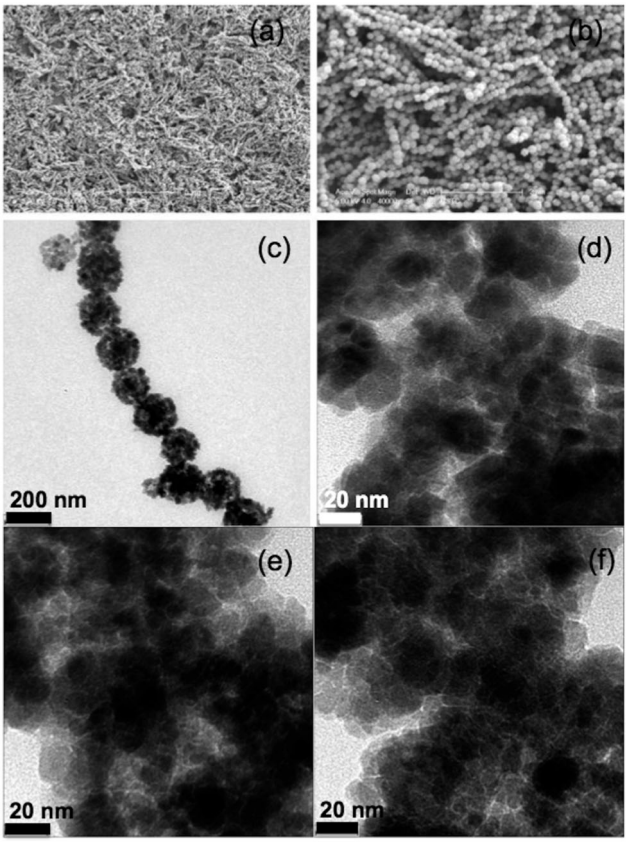

Fig. 2 SEM (a, b) and TEM (c–f) images of the Fe_3O_4 hollow chains reacted for 12 h. The hollow nanospheres are strongly adhered. The formation of the chain bundles is caused by supramolecular hydrogen-bond interactions between the chains and the polyacrylamide surface.

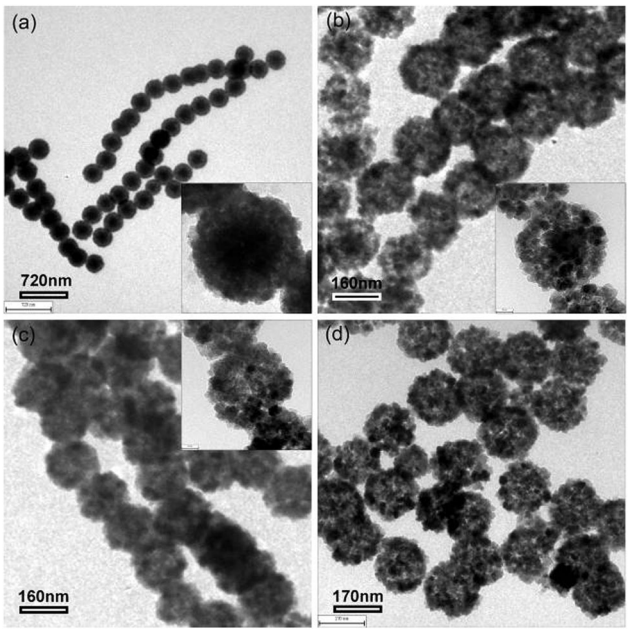

Fig. 3 TEM images of the Fe_3O_4 chains synthesized at different periods of time: 5 h ((a), partially hollow), 12 h ((b), hollow), and 24 h ((c), hollow). (d) TEM image of the individual Fe_3O_4 hollow spheres.

Herein, inter-particle spaces are not observed, revealing that the chains were strongly adhered and the Fe_3O_4 crystals of the surfaces of two hollow spheres were overlapped. These chains were found to be stable even after a high-intensity ultrasonic treatment, proving that the Fe_3O_4 hollow spheres were tightly connected but not through a surface reversible and physical self-assembly (Fig. 3).

Similarly, non-hollow Fe_3O_4 chains can be prepared according to the magnetic field-induced method. Since the above system is not suitable for the non-hollow Fe_3O_4 particles, a mixed solvent method was introduced.[46] Here, $FeCl_3$ and sodium acetate were first dissolved in the EG/DEG at a ratio of 4 : 1. Polyacrylic acid (PAA) acts as a polymer stabilizer. After a hydrothermal reaction in the presence of a magnetic field, Fe_3O_4 chains that are composed of tens of nanospheres were successfully prepared (Fig. 4a and b, Fig. S3 and S4, ESI†). Different from a previous report,[30] the prepared chains were assembled without any inter-particle gap between the Fe_3O_4 nanospheres. The higher magnification TEM image indicates that the Fe_3O_4 nanospheres are peripherally attached instead of an aggregation (inset of Fig. 4b). During the synthesis, the magnetic field induced the formation of the chain structure due to the magnetic dipolar interaction of these Fe_3O_4 nanospheres whereas the two poles of each sphere are more reactive. These Fe_3O_4 nanospheres in the chains presented the cluster-like structures, in which the poly(acrylate) (PA) bonds together at the interfaces of the ultrasmall primary Fe_3O_4 nanograins of the nanospheres.[47,48] Therefore, these Fe_3O_4 nanospheres were gathered to form the head-to-tail configuration since the PAA was tightly connected in the ultrasmall primary Fe_3O_4 nanograins between the nearby two Fe_3O_4 nanospheres.

The as-prepared Fe_3O_4 hollow nanospheres and their chains possessed the same crystal structure, which have been characterized by XRD (Fig. S5, ESI†).[45,48] These hollow nanospheres and chains possess a similar primary nanostructure, thus it is estimated that they will have similar magnetic properties. Fig. S6 (ESI†) shows the *M–H* curves of the as-prepared hollow nanospheres (12 h) and the chains reacted for 5 and 12 h. Clearly, the curves are almost identical for the two materials reacted for 12 h. The coercivity (H_c) and remanent magnetization (M_r) of these particles were almost zero, indicating a typical superparamagnetic characteristic.[47] Therefore, they can be well dispersed to form a homogenous solution and retaining zero residue magnetism without applying the magnetic field. Both the hollow Fe_3O_4 nanospheres and chains can be completely saturated at 1 T magnetic fields with a saturation magnetization (M_s) value of 69.0 and 68.7 emu g^{-1}, respectively. In consideration of the chains obtained after 5 h which were composed of an amorphous Fe-complex precursor, the M_s value is lowered to 41 emu g^{-1}.

These superparamagnetic Fe_3O_4-based hierarchical structures can be easily dispersed to form stable aqueous solutions. By fixing the weight ratio of all Fe_3O_4-based structures at 10 wt%, superparamagnetic aqueous fluids were prepared based on the hollow nanospheres and chains. The commercially available magnetorheometer (Physica MCR 301, Anton Paar, Austria) was used to investigate the shear behaviors of the superparamagnetic fluids. The magnetic field was applied normally to the sample

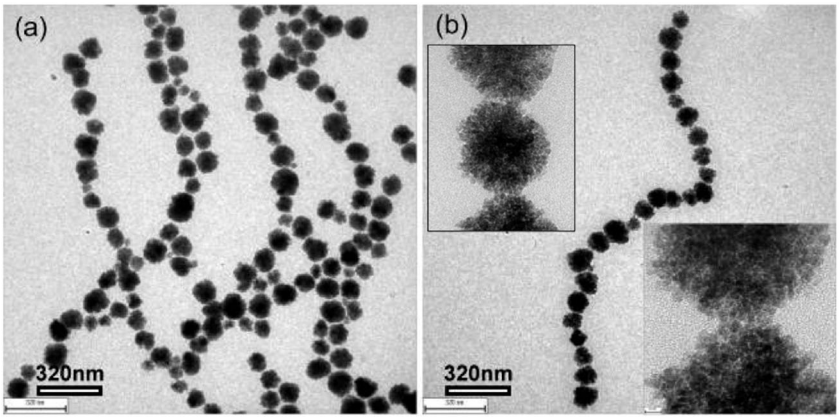

Fig. 4 TEM images of Fe_3O_4 chains based on non-hollow nanospheres synthesized with the magnetic field.

plate *via* the magnetorheological unit (Physica MRD 180) (Fig. S7, ESI†). Before data collection, the superparamagnetic fluids were sheared constantly at the rate of 100 s^{-1} at zero field for 30 s to ensure the homogeneity of the dispersion. Fig. 5a shows the results of the Fe_3O_4 hollow nanosphere-based superparamagnetic fluid. Similar to traditional magnetic fluids, the shear stress increased upon increasing the shear rate, indicating that the Fe_3O_4 hollow nanosphere with an applied magnetic field was continuously broken by the shear deformation.[49] Furthermore, the chains formed by the partially hollow nanospheres (Fig. 5b) and hollow nanospheres (Fig. 5c) with an applied magnetic field were continuously broken by the shear deformation. However, at a high magnetic field (720 and 960 mT), the shear stress values fluctuated possibly because of their intertwined chain structures.

Fig. 5d shows the magnetic field-dependent shear stress of the superparamagnetic fluids composed of hollow nanospheres (12 h), chains of hollow nanospheres (12 h), and chains of partially hollow nanospheres (5 h). A minimal magnetic field strength (120 mT) was required such that the shear stress rapidly increased and the shear stress was about 10–20 times larger (13 Pa for the hollow spheres and 20 Pa for the chains) than that in the absence of the magnetic field. These results prove directly the presence of the magnetorheological effects. Furthermore, the two different chains possess higher shear stress than that of the individual spheres at 120 mT. Upon further increasing the magnetic field from 250 mT to 500 mT, the shear stress decreased, which is in agreement with the results shown in Fig. 5a–c. It was found that these Fe_3O_4 hollow

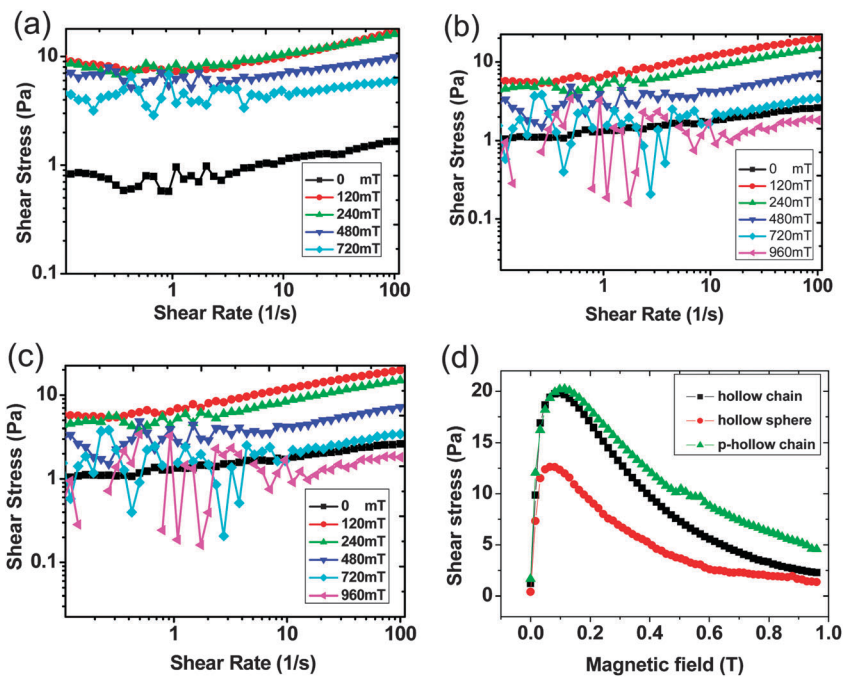

Fig. 5 The shear stress *vs.* shear rate curves of the superparamagnetic fluids based on the Fe_3O_4 hollow nanospheres (12 h) (a) and chains reacted for 5 h (b) and 12 h (c), respectively. (d) The magnetic field dependency shear stress of the superparamagnetic fluids prepared by Fe_3O_4 chains based on hollow nanospheres (hollow chain), the hollow nanospheres, and the Fe_3O_4 chains based on partially hollow nanospheres (p-hollow chain).

nanospheres could be nearly saturated at 240 mT (a shear stress of ~10 Pa at a shear rate of 100 s^{-1}) while the chains could be nearly saturated at 120 mT (a shear stress of ~10 Pa at a shear rate of 100 s^{-1}). Thus the increment of the magnetic dipole inducing forces in the fluid became very small after an increase of the magnetic field. Moreover, since the concentration of all samples is quite low (10 wt%), the particles might gather preferentially in the center of the plate with an externally applied magnetic field. This sealing effect inevitably occurs due to the low viscosity of water.[50] Therefore, the number of the magnetic field-induced nanosphere-based chains which connected the upper and lower plates decreased due to a high magnetic field, thereby also decreasing the shear stress.

In comparison to the hollow nanospheres, the shear stress for the chains is much higher, which indicates that the chains exhibit higher magnetorheological effects. It was reported that magnetic particles could assemble to form wire-like aggregations with the magnetic field thereby increasing the viscosity of the fluids with a magnetorheological phenomenon.[51] In shear analysis, these chains could be continuously broken and re-assembled. Clearly, the chains are more stable than the magnetically induced pseudo-chain structures. Moreover, the bundle wire-like aggregations composed of the Fe_3O_4 chains are even more stable[17] than the chains themselves. Therefore, the fluids based on Fe_3O_4 chains exhibit larger magnetorheological effects than the nanospheres. Since the chains and the hollow nanospheres have the same magnetic properties, the enhancing magnetorheological effects must be correlated with their specific structures.

Somewhat interestingly, the chains based on partially hollow Fe_3O_4 nanospheres (Fig. 5d, green curve) also exhibit a higher magnetorheological effect than the hollow nanospheres (Fig. 5d, black curve) themselves. Although the saturated magnetization of the partially hollow Fe_3O_4 chains is lower than the Fe_3O_4 hollow chains and hollow nanospheres, they have a much larger particle size and a longer chain length. It is estimated that their bundle wire-like aggregations should be stronger than the other two, so the shear stress is larger. Because of their smaller magnetic saturation and longer chain length, the sealing effects may be weaker. Therefore, they exhibit a much higher shear stress when the magnetic field increases to 1 T.

Thermogravimetric analysis at 50 to 700 °C (Fig. 6a) demonstrates the temperature-dependent weight losses of hollow nanospheres and the chains based on hollow nanospheres. The significant weight losses at 200 to 300 °C demonstrate the removal of the organic polymer fractions in the structures. The chains based on hollow nanospheres show higher weight loss (1% at 150–200 °C and 2% at 400–600 °C) than the hollow spheres. This is possibly because in the chains, there are more polymer fractions at the connections between individual spheres, contributing to the weight loss difference at 400–600 °C. Furthermore, water molecules might be trapped inside the bundle-wire structures based on the chains, contributing to the weight loss difference at 150–200 °C.

In Fig. 6b, the chains based on non-hollow Fe_3O_4 nanospheres also exhibit a higher magnetorheological effect than the non-hollow nanospheres themselves from which they showed their maximum shear stress values at 120 mT. It was found that (Fig. 6c) Fe_3O_4 non-hollow nanospheres could be nearly saturated at 120 mT (a shear stress of ~1.5 Pa at a shear rate of 100 s^{-1}) while the chains based on non-hollow nanospheres

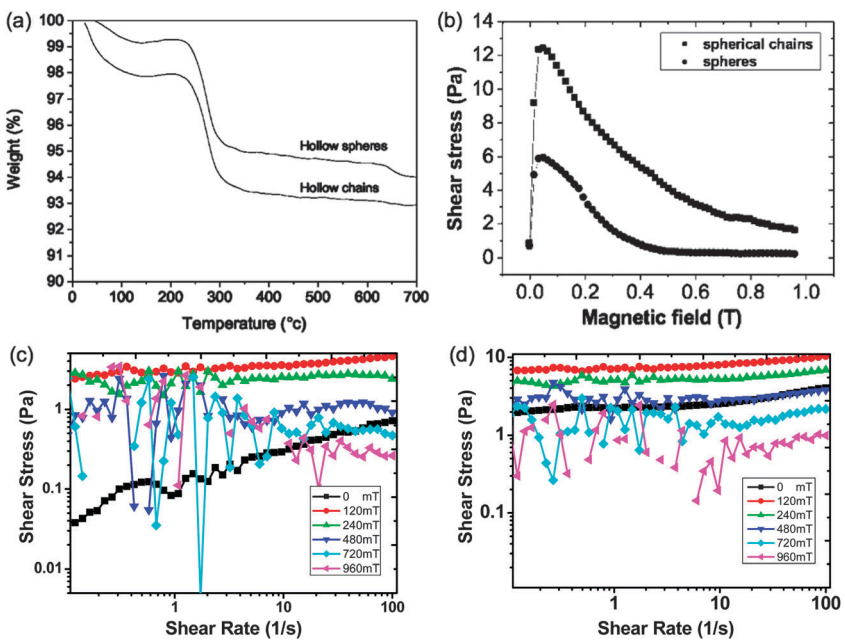

Fig. 6 (a) Thermogravimetric analyses of individual hollow spheres and chains based on hollow spheres (hollow chains). (b) The magnetic field dependency shear stress of the magnetic fluids with Fe_3O_4 chains based on non-hollow nanospheres (spherical chains) and the non-hollow nanospheres (spheres). (c) Shear stress *vs.* rate curves of the superparamagnetic fluids with Fe_3O_4 non-hollow nanospheres. (d) Shear stress *vs.* rate curves of the superparamagnetic fluids with Fe_3O_4 chains based on non-hollow nanospheres.

(Fig. 6d) could be nearly saturated at 120 mT (a shear stress of ~10 Pa at a shear rate of 100 s^{-1}). The Fe_3O_4 chains based on non-hollow nanospheres show a much higher shear stress than the Fe_3O_4 non-hollow nanospheres, demonstrating reasonable results in analyzing the structure–rheology property relationships. Since supramolecular interactions are solvent dependent, it is reasonable to conclude that the chain structures in different dispersing phases play important roles in determining their rheological properties. When the hollow nanospheres were dispersed within an aqueous solution, dispersion was homogenous. When a magnetic field was applied, the Fe_3O_4 hollow nanospheres were magnetically polarized and act as tiny magnets. Due to the magnetic polar–polar forces, these hollow nanospheres were compacted along the magnetic field direction to form bundle wire-like structures. If shear deformation was conducted on these superparamagnetic fluids, the bundle wires could be continuously broken and reassembled until equilibrium is reached. The tested stress under this semi-stable state is the shear stress. For the dispersion phase of Fe_3O_4 chains, they can also assemble to form the bundle wire-like structure due to the presence of the magnetic field. Since the interactions between the hollow nanospheres and the Fe_3O_4 chains are much higher than the magnetic inducing forces because of the friction, blocking, and the water encapsulation in the hollow nanostructures, this novel class of chain-assembled, bundle wire-like structures could be more steady.[14] Therefore, a larger shear force could be required to maintain an equilibrium state such that an enhanced magnetorheological effects was observed.

4. Conclusion

Supramolecular [N–H···C–O] amide hydrogen bond interactions between bundles of necklace-like chains based on superparamagnetic hollow Fe_3O_4 nanoparticle beads have been indirectly quantified by shear stress and magnetorheological analyses. Superparamagnetic Fe_3O_4 necklace chains that are assembled by hollow nanosphere primary units have been developed by using a one-step magnetic field-induced synthetic method. The inner nanostructure of the chains can be tuned by reactions at different times. The superparamagnetic fluids that are prepared by using both the Fe_3O_4 chains and hollow nanospheres in the dispersing phase exhibit a maximum shear stress with an externally applied magnetic field. The Fe_3O_4 chains showed a higher shear stress value than the hollow nanospheres. The structural observation indicates that the magnetically induced bundle wire-like structures assembled from the Fe_3O_4 chains are much more stable than those of the hollow nanospheres. The friction, blocking, and the water encapsulation in the hollow nanostructure greatly strengthen the as-formed bundle wire-like structures, and thus the chains have a larger magnetorheological effect than that of the hollow nanospheres. The hollow nature of our products affects the intrinsic properties compared to non-hollow particles reported elsewhere. The superparamagnetic and hollow nature could possess good magnetic saturation values which further endow them for potential applications as drug carriers and as colloidal probes for measuring the viscoelasticity and magnetic resonance imaging[52] of biological media in living cells. The magnetorheology studies of chains and bundles in this work would shed light on the study of how magnetic field strength affects the cellular uptake with Fe_3O_4 necklace chains in cell magnetofection.

Acknowledgements

We acknowledge financial support from the National Natural Science Foundation of China (Grant No. 11102202), Anhui Provincial Natural Science Foundation of China (1408085QA17), HKRGC-GRF (201412), and University Grants Committee of Hong Kong SAR (AoE/P-03/08).

References

1 K. C.-F. Leung, S. H. Xuan, X. M. Zhu, D. W. Wang, C.-P. Chak, S.-F. Lee, W. K.-W. Ho and B. C.-T. Chung, *Chem. Soc. Rev.*, 2012, **41**, 1911–1928.
2 Y. Pan, X. W. Du, F. Zhao and B. Xu, *Chem. Soc. Rev.*, 2012, **41**, 2912–2942.
3 R. A. Frimpong and J. Z. Hilt, *Nanomedicine*, 2010, **5**, 1401–1414.
4 Y. X. J. Wang, X.-M. Zhu, Q. Liang, C. H. K. Cheng, W. Wang and K. C.-F. Leung, *Angew. Chem., Int. Ed.*, 2014, **53**, 4812–4815.
5 K. C.-F. Leung, C.-P. Chak, S.-F. Lee, J. M. Y. Lai, X.-M. Zhu, Y.-X. J. Wang, K. W. Y. Sham and C. H. K. Cheng, *Chem. Commun.*, 2013, **49**, 549–551.
6 K. C.-F. Leung, C.-H. Wong, X.-M. Zhu, S.-F. Lee, K. W. Y. Sham, J. M. Y. Lai, C.-P. Chak, Y.-X. J. Wang and C. H. K. Cheng, *Quant. Imaging Med. Surg.*, 2013, **3**, 302–307.
7 K. C.-F. Leung, S.-F. Lee, C.-H. Wong, C.-P. Chak, J. M. Y. Lai, X.-M. Zhu, Y.-X. J. Wang, K. W. Y. Sham and C. H. K. Cheng, *Methods*, 2013, **64**, 315–321.
8 K. C.-F. Leung, C.-P. Chak, S.-F. Lee, J. M. Y. Lai, X.-M. Zhu, Y.-X. J. Wang, K. W. Y. Sham, C.-H. Wong and C. H. K. Cheng, *Chem. – Asian J.*, 2013, **8**, 1760–1764.
9 K. C.-F. Leung, Y.-X. J. Wang, H. Wang, S. H. Xuan, C.-P. Chak and C. H. K. Cheng, *IEEE Trans. Nanobiosci.*, 2009, **8**, 192–198.
10 Y. J. Kim, Y. D. Liu, Y. Seo and H. J. Choi, *Langmuir*, 2013, **29**, 4959–4965.
11 Y. Pan, Y. Gao, J. F. Shi, L. Wang and B. Xu, *J. Mater. Chem.*, 2011, **21**, 6804–6806.
12 X. Y. Qiao, J. Zhou, P. B. Bernard, X. L. Gong and K. Sun, *Colloids Surf., A*, 2012, **412**, 20–28.
13 A. Gomez-Ramirez, M. T. Lopez-Lopez, J. D. G. Duran and F. Gonzalez-Caballero, *Soft Matter*, 2009, **5**, 3888–3895.
14 R. C. Bell, E. D. Miller, J. O. Karlf, A. N. Vaverck and D. T. Zimmerman, *Int. J. Mod. Phys. B*, 2007, **21**, 5018–5025.
15 Z. M. Yang, H. W. Gu, J. Du, J. H. Gao, B. Zhang, X. X. Zhang and B. Xu, *Tetrahedron*, 2007, **63**, 7349–7357.
16 M. T. Lopez-Lopez, G. Vertelov, G. Bossis, P. Kuzhir and J. D. G. Duran, *J. Mater. Chem.*, 2007, **17**, 3839–3844.

17 R. C. Bell, J. O. Karli, A. N. Vavreck, D. T. Zimmerman, G. T. Ngatu and N. M. Wereley, *Smart Mater. Struct.*, 2008, **17**, 015028.
18 S. H. Xuan, Y. X. J. Wang, J. C. Yu and K. C.-F. Leung, *Chem. Mater.*, 2009, **21**, 5079–5087.
19 W. H. Chong, L. K. Chin, R. L. S. Tan, H. Wang, A. Q. Liu and H. Y. Chen, *Angew. Chem., Int. Ed.*, 2013, **52**, 8570–8573.
20 Y. Pan, M. J. C. Long, H. C. Lin, L. Hedstroma and B. Xu, *Chem. Sci.*, 2012, **3**, 3495–3499.
21 C. Galindo-Gonzalez, M. T. Lopez-Lopez and J. D. G. Duran, *J. Appl. Phys.*, 2012, **112**, 043917.
22 K. Nakata, Y. Hu, O. Uzun, O. Bakr and F. Stellacci, *Adv. Mater.*, 2008, **20**, 4294–4299.
23 B. Y. Geng, F. M. Zhan, H. Jiang, Y. J. Guo and Z. J. Xing, *Chem. Commun.*, 2008, 5773–5775.
24 G. F. Zou, K. Xiong, C. L. Jiang, H. Li, T. W. Li, J. Du and Y. T. Qian, *J. Phys. Chem. B*, 2005, **109**, 18356–18360.
25 J. Lu, X. L. Jiao, D. R. Chen and W. Li, *J. Phys. Chem. C*, 2009, **113**, 4012–4017.
26 F. A. Harraz, *Phys. E*, 2008, **40**, 3131–3136.
27 R. Sheparovych, Y. Sahoo, M. Motornov, S. M. Wang, H. Luo, P. N. Prasad, I. Sokolov and S. Minko, *Chem. Mater.*, 2006, **18**, 591–593.
28 J. Wang, Q. W. Chen, C. Zeng and B. Y. Hou, *Adv. Mater.*, 2004, **16**, 137–139.
29 A. Ahniyaz, Y. Sakamoto and L. Bergstrom, *Proc. Natl. Acad. Sci. U. S. A.*, 2007, **104**, 17570–17574.
30 F. Vereda, J. D. Vicente and R. Hidalgo-Alvarez, *Colloids Surf., A*, 2008, **319**, 122–129.
31 H. Wang, Q. W. Chen, L. X. Sun, H. P. Qi, X. Yang, S. Zhou and J. Xiong, *Langmuir*, 2009, **25**, 7135–7139.
32 C. J. Jia, L. D. Sun, F. Luo, X. D. Han, L. J. Heyderman, Z. G. Yan, C. H. Yan, K. Zheng, Z. Zhang, M. Takano, N. Hayashi, M. Eltschka, M. Klaui, U. Rudiger, T. Kasama, L. Cervera-Gontard, R. E. Dunin-Borkowski, G. Tzvetkov and J. Raabe, *J. Am. Chem. Soc.*, 2008, **130**, 16968–16977.
33 S. H. Xuan, L. Y. Hao, W. Q. Jiang, L. Song, Y. Hu, Z. Y. Chen, L. F. Fei and T. W. Li, *Cryst. Growth Des.*, 2007, **7**, 304–307.
34 Z. Q. Liu, D. H. Zhang, S. Han, C. Li, B. Lei, W. G. Lu, J. Y. Fang and C. W. Zhou, *J. Am. Chem. Soc.*, 2005, **127**, 6–7.
35 H.-F. Chow, C.-F. Leung, W. Li, K.-W. Wong and L. Xi, *Angew. Chem., Int. Ed.*, 2003, **42**, 4919–4923.
36 H. D. A. Mohamed, S. M. D. Watson, B. R. Horrocks and A. Houlton, *Nanoscale*, 2012, **4**, 5936–5945.
37 Y.-X. J. Wang, S. H. Xuan, M. Port and J. M. Idee, *Curr. Pharm. Des.*, 2013, **19**, 6575–6593.
38 S. Shen, F. F. Kong, X. M. Guo, L. Wu, H. J. Shen, M. Xie, X. S. Wang, Y. Jin and Y. R. Ge, *Nanoscale*, 2013, **5**, 8056–8066.
39 S. H. Hu and X. H. Gao, *J. Am. Chem. Soc.*, 2010, **132**, 7234–7237.
40 S. H. Xuan, F. Wang, J. M. Y. Lai, K. W. Y. Sham, Y.-X. J. Wang, S.-F. Lee, J. C. Yu, C. H. K. Cheng and K. C.-F. Leung, *ACS Appl. Mater. Interfaces*, 2011, **3**, 237–244.
41 S. H. Xuan, F. Wang, X. L. Gong, S.-K. Kong, J. C. Yu and K. C.-F. Leung, *Chem. Commun.*, 2011, **47**, 2514–2516.
42 B. Wang, H. B. Wu, L. Zhang and X. W. D. Lou, *Angew. Chem., Int. Ed.*, 2013, **52**, 4165–4168.
43 S. Xu, B. R. Yin, J. Guo and C. C. Wang, *J. Mater. Chem. B*, 2013, **1**, 4079–4087.
44 R. J. Xing, A. A. Bhirde, S. J. Wang, X. L. Sun, G. Liu, Y. L. Hou and X. Y. Chen, *Nano Res.*, 2013, **6**, 1–9.
45 S. H. Xuan, Y. F. Zhou, H. J. Xu, W. Q. Jiang, K. C.-F. Leung and X. L. Gong, *J. Mater. Chem.*, 2011, **21**, 15398–15404.
46 X. M. Zhu, J. Yuan, K. C.-F. Leung, S.-F. Lee, K. W. Y. Sham, C. H. K. Cheng, D. W. T. Au, G. J. Teng, A. T. Ahuja and Y.-X. J. Wang, *Nanoscale*, 2012, **4**, 5744–5754.
47 S. H. Xuan, S.-F. Lee, J. T.-F. Lau, X. M. Zhu, Y.-X. J. Wang, F. Wang, J. M. Y. Lai, K. W. Y. Sham, P.-C. Lo, J. C. Yu, C. H. K. Cheng and K. C.-F. Leung, *ACS Appl. Mater. Interfaces*, 2012, **4**, 2033–2040.
48 W. Cheng, K. B. Tang, Y. X. Qi, J. Sheng and Z. P. Liu, *J. Mater. Chem.*, 2010, **20**, 1799–1805.
49 M. Sedlacik, V. Pavlinek, R. Vyroubal, P. Peer and P. Filip, *Smart Mater. Struct.*, 2013, **22**, 035011.
50 C. Y. Guo, X. L. Gong, S. H. Xuan, Q. F. Yan and X. H. Ruan, *Smart Mater. Struct.*, 2013, **22**, 045020.
51 B. J. Park, F. F. Fang and H. J. Choi, *Soft Matter*, 2010, **6**, 5246–5253.
52 X.-M. Zhu, Y.-X. J. Wang, K. C.-F. Leung, S.-F. Lee, F. Zhao, D.-W. Wang, J. M. Y. Lai, C. Wan, C. H. K. Cheng and A. T. Ahuja, *Int. J. Nanomed.*, 2012, **7**, 953–964.

